A Novel Fiber-Bragg-Grating-Based Unique Identifier for Use in Tags and Seals

Klaus-Peter Ziock, Philip Evans, Brandon Longmire, Will Ray, James Younkin
Oak Ridge National Laboratory[1]
PO Box 2008, MS-6166, Oak Ridge, TN 37831-6166

Abstract

Tags and seals are important tools used in safeguards regimes for the control of nuclear materials. Vital to a successful tag or seal is the ability to securely, uniquely, and positively distinguish it from others of the same kind. This allows one to validate that items entered into an inspection regime to which the tag or seal is affixed are as claimed. We are developing a new type of unique identifier (UID) for such applications that is based on fiber-Bragg grating (FBG) technology. FBGs are passive optical devices written into the core glass of fiber optics that block narrow spectral bands of light in resonance with their design. Instead of transmission, the resonant light is reflected back in the direction it came. An optical interrogator can be used to measure spectral signatures returned by the FBGs, allowing one to make the unique identification. As a device based on narrowband spectral returns, FBGs are inherently radiation tolerant, making them ideal for use with nuclear materials. Further, they can be read out remotely via a long fiber optic, or locally via brief connection to a portable optical interrogator. Because the spectral signature of FBGs is sensitive to external mechanical perturbations, we are exploring the ability to reversibly alter the signature obtained from the UID by applying controlled mechanical forces with a simple device. Such a "key" will allow different stakeholders to obtain their own unique signature from the device, providing a new level of surety to safeguards inspections.

Introduction

Tags and seals have been used throughout human history. A simple example of an early seal is the signet ring (Fig. 1) that is used to emboss a user's ID onto wax used to seal an envelope. Even earlier systems based on impressions in clay are well documented [1]. Today many passive tags and seals rely on the same simple precept of attaching something to the item to be 'secured' and looking for changes to that something as in indication of tampering. Typically, seals include a component that will break if the seal is tampered with, and a unique identifier that is difficult to reproduce, yet is easily identified. A seal's function is to register unauthorized access to the contents of the monitored item by recording a detectable change to the seal. Note that this is not the same function provided by a lock, which is meant to slow unauthorized access to an item. At the heart of this approach are UIDs, and these take many forms (Fig. 1) from uniquely marked, frangible stickers that disintegrate on access, to objects that have unique randomized patterns (such as complex scratch patterns), inside sealed components that must be (destructively) opened for access. There are also active approaches that include sensing current fields in membranes

[1] This manuscript has been authored by UT-Battelle, LLC, under contract DE-AC05-00OR22725 with the US Department of Energy (DOE). The US government retains and the publisher, by accepting the article for publication, acknowledges that the US government retains a nonexclusive, paid-up, irrevocable, worldwide license to publish or reproduce the published form of this manuscript, or allow others to do so, for US government purposes. DOE will provide public access to these results of federally sponsored research in accordance with the DOE Public Access Plan (http://energy.gov/downloads/doe-public-access-plan).

surrounding an object, and continuously monitored fiber optics that must be broken (or stressed) during access. A full review of the field is well beyond the scope of this document, and the interested reader is referred to [1] for a brief overview of the topic as applicable to nuclear materials management.

Fig. 1. From left to right, Signet ring circa 1570 for the town of Náchod [2]. IAEA seals: metal cap seal, COBRA seal and an electronic optical sealing system (EOSS) [3].

Fiber Bragg Gratings

Fiber Bragg gratings (FBG) [4] are optical devices written into optical glass fibers using intense UV light to create small, permanent spatial changes in the index of refraction of the fiber core (Fig. 2). Typically, the changes are written with a regular periodicity commensurate with the wavelength of the light sent down the fiber. The resulting optical structure acts as a Bragg reflector for incident light in resonance with the structure, returning the light back through the fiber where it can be detected. A typical response from a uniform FBG (Fig. 3) has sidelobes that add spectral complexity to the reflected spectrum. These can be suppressed by varying the intensity of the pattern written into the fiber core at the beginning and end of the FBG. Such "apodized" gratings provide a cleaner return with a central reflection wavelength that can be monitored autonomously to look for changes in the wavelength.

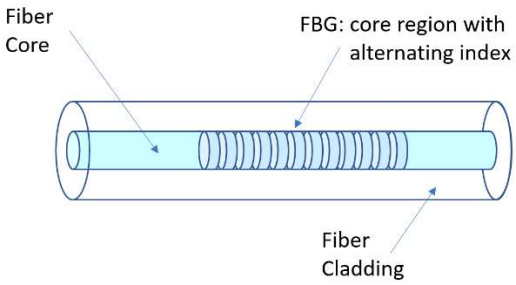

Fig. 2. Schematic of an FBG with the index of refraction of the core of a fiber optic varied as a function of location.

A FBG's periodicity (grating spacing) will be altered by changes in external parameters such as temperature, tension, and pressure, allowing their use as sensors to monitor for changes in these parameters. In fact, by building the FBGs into mechanical structures, sensitive sensors can be designed that monitor for specific external parameters. For instance, they are widely used in civil engineering to monitor structural stresses [5]. FBGs have several advantages over electro-mechanical systems including longevity and robustness. Their lack of an electrical signal also means that they are free from electrical interference, and they may be used for long-distance remote monitoring because of the ability to transmit light long distances through fiber optics. The localized nature of the spectral response also provides robustness against radiation damage which generates broadband attenuation in fiber optics via yellowing. As evidence for this, FBGs have been used in the high radiation fields of the Compact Muon Solenoid experiment at CERN [6]. Finally, spectral shifts are much easier to track than absolute amplitude measurements.

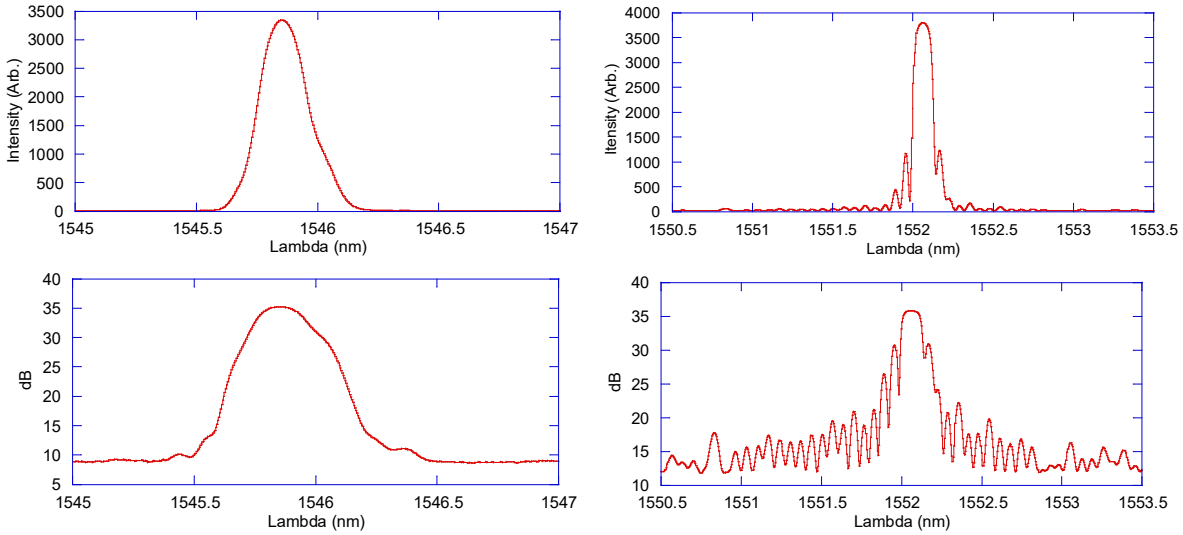

Fig. 3. Normalized spectra returned by an apodized (left) and uniform (non-apodized) FBG (right). The upper row shows the linear response, whereas the lower row is given in decibels, accentuating side-lobe structure.

UID Design

The overall concept for the UID under development includes one or more FBGs that are written into the same fiber optic. The fiber is coiled into a well (Fig. 4) where it is potted into place, both for protection and to eliminate the chance of tampering with the fiber. Before potting, the fiber is passed through a hole in the body of a standard cable seal closure that fits in a slotted compartment within the device. The short lengths of fiber optic on either side of the cable seal body (CSB) are too short to allow reconnecting the ends of the fiber to restore the optical path if the fiber is broken by attempting to replace the cable seal. Hence, once the cable seal is engaged, the only way to remove it from a monitored item is to cut the cable, a clear indication that tampering has occurred. To further discourage tempering with the seal, the CSB compartment is long enough to allow the CSB to move if one pulls on the cable and break the fiber optic. Again, this provides a clear indication that the device had been tampered with. To keep the CSB from sliding during standard usage, a thin member is used to retain the CSB in location. The member is designed so that excessive force applied to the cable will snap the member (current breaking force 15-20 kg), allowing the CSB to slide, thereby breaking the optical fiber.

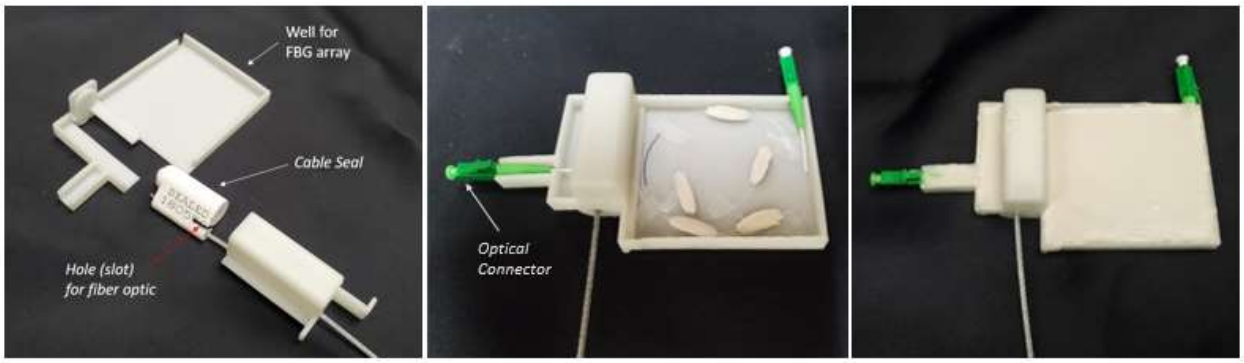

Fig. 4, UID assembly. Left, the mechanical components of the UID. Center, the mechanical components assembled with the FBG (pre-potted, see text) array distributed in the well for final potting. Right, The completed assembly.

The potting material is an important component of the design concept; however, it can induce stresses on the FBGs that cause the spectral return to change. Stresses arise from dimensional changes when the potting material sets, and from mismatches between the coefficients of thermal expansion (CTE) of the various materials used in the fiber-optic itself [7], the potting compound, and the body into which the UID is potted. In the end, the goal is to create a potted UID with a signature that is either invariant or reproducible with temperature. Significant experimentation was required to develop a technique that met this requirement. Good results were finally achieved by pre-potting just the FBG segments of the FBG array in a straight configuration after application of a release agent. This is the reason for the white oval shaped potting material seen in the center image of Fig 4., before the FBG array is potted into the well.

Spectral Analysis

At the heart of the new device is the ability to provide a unique identifier (UID) that has the following characteristics: Provides a globally unique identification, is difficult to counterfeit (even with the resources of a state actor), is easy to verify in situ, is radiation tolerant, and does not rely on visual imagery. To accomplish these goals requires not just a unique spectral return, but a readout device and analysis procedure that can provide definitive results in real time.

Because FBGs are widely used for civil engineering, a number of small, sensitive, optical interrogators used to readout the devices are available commercially. For our application, where we wish to identify an FBG over a broad spectral range, we are concerned with spectral resolution and selected a swept, pulsed, laser system [8] that provides spectra over a range of 1529 nm to 1568.2 nm with picometer resolution at a rate of 4 Hz, allowing us to map the spectral return from multiple FBGs simultaneously. To readout the UID, it is connected to the optical interrogator and ~ 40 spectra are collected and averaged for analysis.

To validate the signature from an FBG, the returned spectrum is compared to stored reference shapes from the device. The reference shapes are saved from the newly manufactured UID at a temperature of 25 C by selecting a region around the reflected signal (Fig. 5). Three statistics are generated for each FBG in an UID, the peak wavelength, the strength of the signal (peak to background), and a difference-correlation, shape parameter, V_{cc} defined as:

$$V_{cc}(\lambda) = \frac{\sum_{i=0}^{n} |S_i - D_{\lambda - i}|}{\#\ Channels} \quad (1)$$

where S_i is the value of the shape at spectral bin i, $D_{\lambda\text{-}I}$ is the normalized spectral data offset by the wavelength of the comparison location, and the entire value is normalized by the number of spectral bins in the shape. This term is identically zero at the wavelength, λ, if the expression is applied to the spectrum from which the shape was harvested (Fig. 6). In general, small spectral

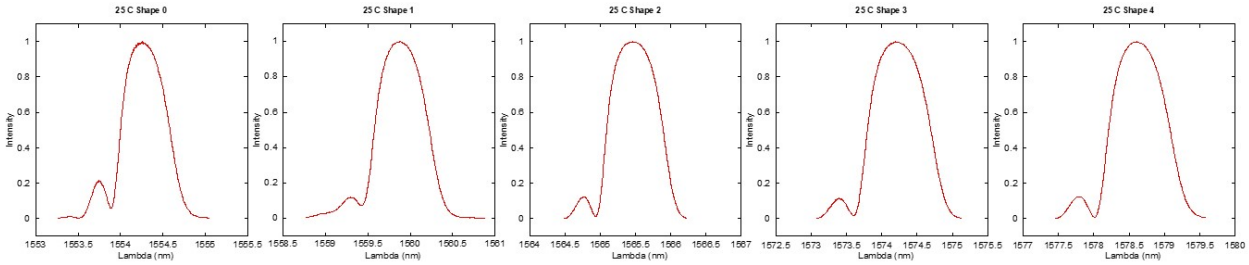

Fig. 5. The five FBG shapes for the UID analyzed in Fig. 8.

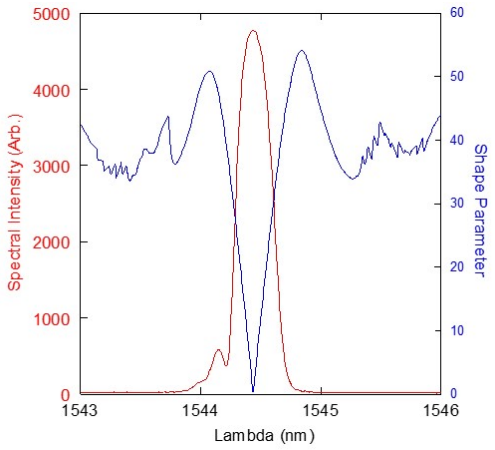

Fig. 6. Sample FBG spectrum and the corresponding Vcc results

shifts and noise means that V_{cc} will go through a non-zero minimum if the expression is applied to a different spectrum from the same FBG.

For an UID that has multiple FBGs, one can calculate a minimum shape for each FBG, $V_{Min}(T)$. one can also calculate an average wavelength $\overline{\lambda}(T)$ from all of the individual FBG wavelengths, $\lambda_i(T)$. Additionally, a useful parameter is a comparison of the offset of each FBG's wavelength from the average compared to the offset for that FBG's wavelength in the reference spectrum:

$$\delta\lambda_i(T) \stackrel{\text{def}}{=} \left(\overline{\lambda}(T) - \lambda_i(T)\right) - (\overline{\lambda}_0 - \lambda_{i0}). \quad (2)$$

Similarly, one can define a fractional shift in the amplitude of each peak in the UID from the peak height of the largest peak, defined as:

$$\delta I_i(T) \stackrel{\text{def}}{=} \left(I_{Max}(T) - I_i(T)\right) - (I_{0Max} - I_{0i}), \quad (3)$$

where the peak amplitude from a given FBG is I, and I_{Max} is the amplitude of the most intense reflection.

Thermal Analysis

Because the temperature, T, impacts the spectral results, all of the values defined above [$V_{Min}(T)$, $\delta\lambda_i(T)$, and $\delta I_i(T)$] are explicitly written as functions of the temperature at which the spectrum being analyzed was collected. For an unconstrained FBG (e.g. unpotted), the primary change in response with temperature is a uniform shift of the shape to longer wavelengths with higher temperatures. This shift is significant and reproducible with gradients of order 1.05×10^{-3} nm/C. Hence, without additional perturbations each FBG acts as a thermometer and the average wavelength from all of the gratings can be used to determine the temperature at which the measurement is taken. While the shape and intensity returned from an unpotted grating do not change significantly with temperature, the changes from potted gratings can be large enough to impact the ability to distinguish different FBGs so an analysis procedure that compensates for this was developed.

If the shape, amplitude, and wavelength variations are reproducible with temperature, then one can harvest a set of reference signatures at multiple temperatures, that are provided to users together with the UID. Analysis of spectral data can then be performed using the reference data closest in temperature to that at which the spectral data were collected. To collect this data, the UIDs are placed in an environmental chamber that is stepped in 5 C increments from -15 to 75 C with 30 min. soak times at each temperature, with spectral data collected every 5 min. (Fig. 7). The next-to-last data taken at 25 C is manually analyzed to select the shapes for all of the FBGs in the UID. An automated routine is then used to harvest the signatures from the next-to-last data acquisition at each of the other soak temperatures in the first thermal cycle. The routine automatically finds each of the peaks in the spectrum and harvests a spectral shape centered on each peak the same way that the original shape at 25 C is centered on its peak (e.g. the number of channels above and below the peak is retained.) The data are then saved with the temperature

linked to the average wavelength from all of the FBGs in the UID. We note that the wavelength of a FBG is determined from the wavelength where the shape value is at a minimum, not from the channel where the peak reflection value occurs.

Analysis of an arbitrary spectrum is performed using the devices reference signatures as follows. A first pass analysis using the 25 C shape data obtains an average wavelength. The reference signatures are searched for the set with the closest average wavelength, and those reference data are used to obtain a revised average wavelength. That wavelength is used to select the reference data set for a final analysis, and those results are reported as the analysis output. This double procedure accounts for small shape changes that can bias the original result to an incorrect temperature, e.g., the use of an incorrect reference data set. A plot of the results from a potted UID as it is cycled through three thermal cycles are given in Fig. 8. The figure also shows the results obtained using only a single reference data set at 25 C. As can be seen, the results obtained with the multi-thermal analysis have smaller variations than those obtained with the single temperature approach.

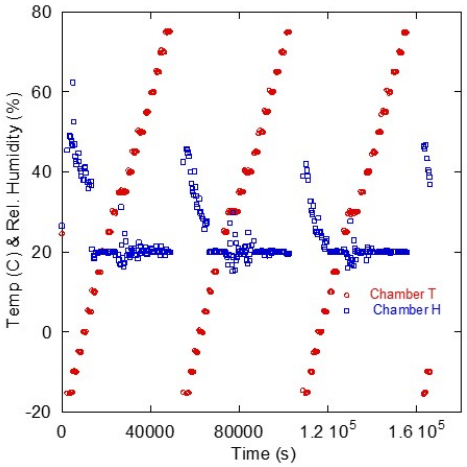

Fig. 7. Environmental chamber conditions versus time for the data shown in Fig. 8

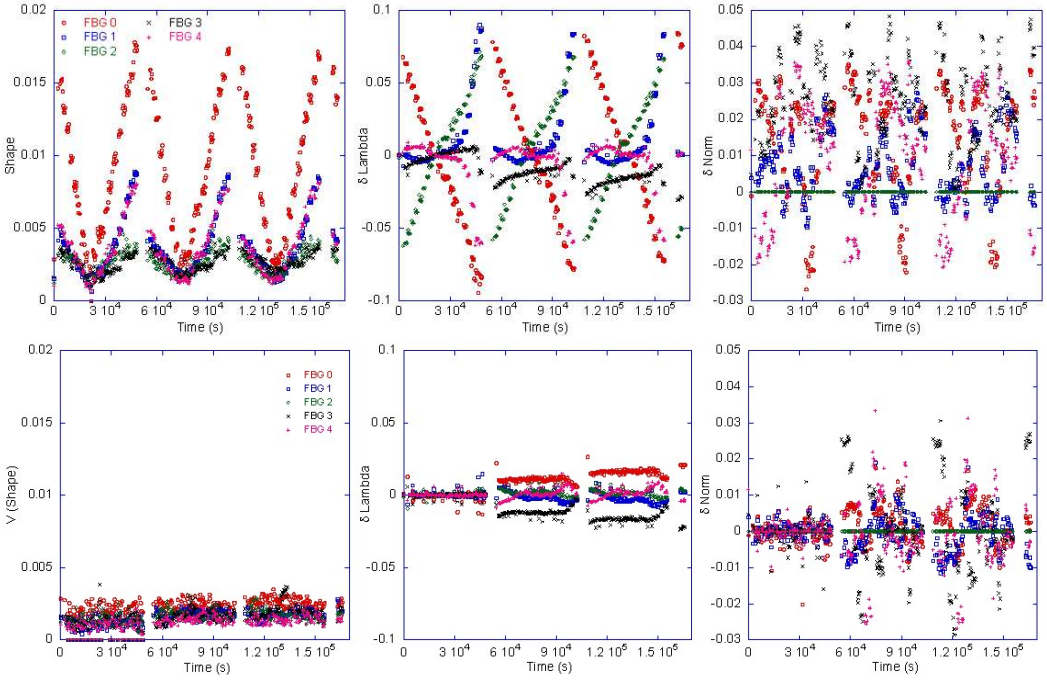

Fig. 8. Individual FBG analysis results from a potted UID as it undergoes three thermal cycles from -15 C to 75 C. (Top row) analysis using shapes from a single temperature (25 C). (Bottom row) analysis using shapes harvested during the first temperature cycle, corresponding to the shape values near zero (see Fig. 6).

Optical Design

To achieve a viable UID requires both having a sufficiently large phase space of discernable signatures so the same signature is not used twice, and having signatures that are difficult to

counterfeit. To address the former, one needs to know how many unique UIDs, M, can be manufactured from a given number, n, of FBGs. A lower estimate can be obtained by calculating the number of distinct spectral locations, p, available within the optical interrogator's bandwidth. One is free to populate any of the spectral locations with an FBG, although the same spectral bin cannot be populated twice. This number is given by the binomial coefficient. In addition, at each spectral location one can select any of k unique FBGs based on their distinguishable reflection intensities. M is then increased by k^n since each location can have k possible FBGs selected. This gives:

$$M \geq \binom{p}{n} k = \frac{p!}{n!(p-n)!} k^n. \quad (4)$$

Opting for an individual FBG spectral bandwidth of 0.25 nm over an interrogator bandwidth of 40 nm gives a total of 160 possible locations. For k an estimate of 13 is given by the ability to distinguish a 3 dB amplitude difference within a 40 dB signal-to-noise ratio. Table 1 shows the minimum number of possible combinations as a function of n. Clearly only a few FBGs are required to achieve a very large number of possible UIDs and we emphasize that this is a significant underestimate since it includes neither the shape parameter, nor the ability to have FBGs with different spectral bandwidths and complexities. For the purposes of the prototype development a virtually infinite phase space based on a 5-FBG array was selected.

Table 1: Number of UIDs

n	M
1	2080
2	2.15×10^6
3	1.47×10^9
4	7.51×10^{11}
5	3.05×10^{14}

Determining the difficulty associated with counterfeiting an UID is complex. In principle, one could simply measure the UID signature and then make a new device by selecting off-the-shelf FBGs with the appropriate signatures. In fact, identical off-the-shelf items do not exist. Even the unconstrained signatures of "identical" FBGs are generally distinguishable by shape, as shown in Figs. 9 and 10, where histograms of shape values obtained both from the self-analysis of an UID and cross-analysis (one UID analyzed with the shape of an "identical" mate) are presented. The data were collected on unpotted UIDs across the operational temperature range of -15 to 75 C using the procedure described above. As can be seen in the left plots of the figures, the values of the shape parameter from the cross analysis are typically much larger than any of the shape values from the self-analysis, although there is some overlap of the results from one of the FBGs. When the product of all FBG shape values is taken (Fig. 9, center), the distributions are clearly separated.

The product of the shapes from self-analyses of five UIDs gave a largest value of 7.6 while the smallest cross-analysis product was 2842 (both multiplied by 10^{15}). This difference provides a comfortable separation, indicating the uniqueness of the different "identical" arrays. In fact, greater separation of the shape values has been obtained using either an edge weighted analysis (progressively weighting those bins of the shape furthest from the central wavelength) and using an analysis where the intensity is given in decibels. Both of those technique weight the shape of the side lobes of the spectrum more heavily than the central peak.

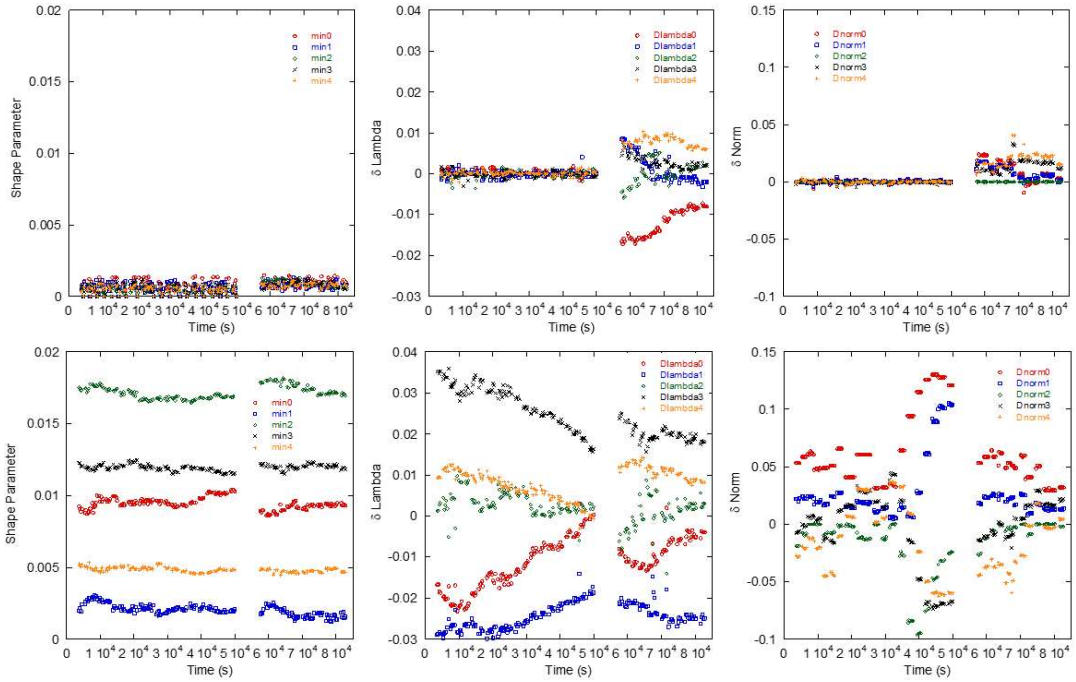

Fig. 9. Self-analysis (upper) results and cross-analysis result (lower) for the unpotted UID shown in Fig. 10.

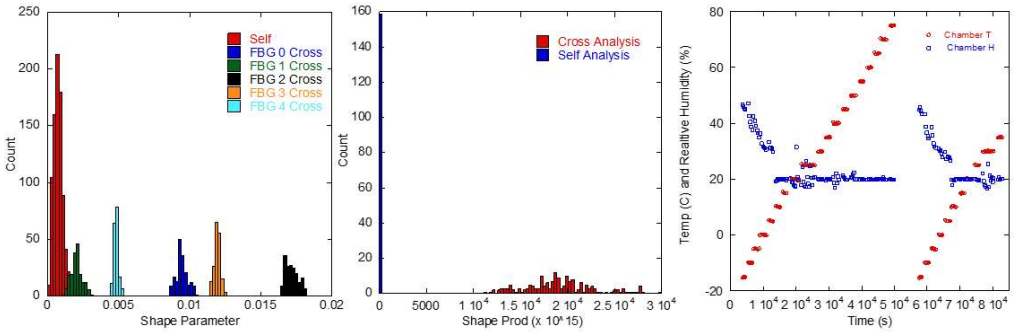

Fig. 10. (Left) Histogram of the shape results from the UID shown in Fig. 9, with the red peak including all FBG self-analysis values and the others the individual FBG cross-analysis values. (Center) The data from the same two analyses treated as the product of the FBG shape values. (Right) Temperature and Humidity as a function of time.

Of course, the real concern is the more complex issue of the uniqueness of the potted FBG arrays. At a minimum, the signatures of the potted FBGs are shifted in wavelength by a uniform strain. The potted signatures also vary with temperature, and finally the key-based signature will depend on the details of how the FBGs are located within the potting compound, with distributions deliberately varied between UIDs. In fact, as mentioned above, much of the difficulty in developing a viable UID has been in developing a potting procedure that yields reproducible results with temperature.

Key Concept and Tests

At the time this paper was prepared, the details of the key design were still under development. However, the concept has been validated with data collected on a potted FBG using a spring-loaded pin normally used for making electrical contacts. The pin was lowered onto the potted FBG and the change in shape recorded as a function of force applied to the pin

(Fig. 11). The results show a repeatable shape change over three cycles. However, there is a small offset in the force required at each cycle, presumably due to the very small contact area of the pin causing some local inelastic deformation of the potting material.

For the final design an array of spring-loaded contacts will be applied to the surface of the potting material encasing the FBG array. Each key will have pins with different pin locations and contact forces, both combining to create a unique stressor field on the UID.

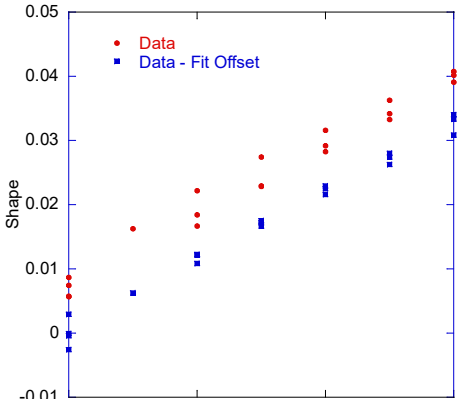

Fig. 11. Shape changes as a function of force induced in a single potted FBG by applying a spring-loaded pin. The blue points include compensation for offset shifts between trials (see text).

Discussion

The use of fiber optics in security is not a new development [9]. However, FBGs provide a new dimension to fiber-optic based technologies by providing a rich and complex signature in a simple device that is ideal for use in a passive UID. With FBGs as building blocks, it is possible to develop a virtually limitless number of unique signatures that are easily validated using the spectral analyses presented above. However, the interests of an inspector are much simpler, desiring only an indication that a given device is the one originally attached to a monitored item. To achieve this will require combining the various signatures into a single indicator; the proverbial red light/green light binary result. It is clear from work to date that the product of the shape parameters from all of the component FBGs can provide such an indicator. However, it will require producing and measuring a larger sample of devices to optimize how the other parameters (δ–Lambda, δ-Norm) can be combined to yield a single statistic with a robust threshold for discovering falsification.

One of the goals of this work was to develop a robust UID that does not require the use of visual imagery for verification because the use of cameras can be an issue at some inspection sites. This device meets that criterium and also other concerns that might arise in some nuclear settings. In particular, the device can be analyzed without requiring an electrical connection. In addition, remote readout is possible as long as an optical connection is maintained. In fact, for monitoring the health of structures in civil engineering, remote readout is an important capability, and interrogators routinely include such analysis tricks as assigning the distance to the FBG based on the roundtrip time of the light from the interrogator to the FBG and back to aid in the analysis.

Finally, the concept of individual keys that allow stakeholders to obtain different signatures from the same device represents an entirely new concept for use in tags and seals. This clearly represents a means of improving the device security since counterfeiting a UID without knowing what the properties of the various keys associated with that device are, make an already difficult task even harder. Beyond this simple function, it will be interesting to see how the user community might take advantage of such a capability.

Conclusion

The FBG-based design is still in the final stages of development and a number of issues remain to be fully addressed to realize a final design. These include completing the mechanical design for the user keys, refining the analysis to provide a red-light/green-light metric, validating the long-term stability of the spectral signatures, and testing the FBG response to high-doses of radiation. Nevertheless, the results to date promise a UID that provides a high degree of security in a device that will be simple to use.

Acknowledgements

The work presented in this paper was funded by the National Nuclear Security Administration of the Department of Energy Office of Defense Nuclear Nonproliferation Research and Development.

References

1. R.G. Johnston, "Tamper-Indicating Seals for Nuclear Disarmament and Hazardous Waste Management," *Sci. & Glob. Sec.*, vol. 9, pp. 93-102, 2001.
2. By Kozuch - Self-photographed, CC BY-SA 3.0, https://commons.wikimedia.org/w/index.php?curid=7971994.
3. *IAEA Bulletin*, p. 19, June 2016, Available from www.iaea.org/bulletin.
4. K. Hill, B. Malo, F. Bilodeau, D. Johnson, and J. Albert, "Bragg gratings fabricated in a monomode photosensitive optical fiber by UV exposure through a phase mask", *Appl. Phys. Lett.*, vol. 62, 10351037, 1993.
5. A. Méndez, "Fiber Bragg grating sensors: A market overview," *Proc. SPIE*, vol. 6619, pp. 661905-6, doi: 0.1117/12.738334.
6. Z.Szillasi, et al., "One year of FOS measurements in CMS experiment at CERN," *Phys. Proc.*, vol 37, pp. 79-84, 2012, doi: 10.1016/j.phpro.2012.02.360.
7. Y. Nakajima, et al., "A Study for Estimating Thermal Strain and Thermal Stress in Optical Fiber Coatings," *Furukawa Review*, No. 34, pp 8-12, 2008. Available: www.furukawa.co.jp/review/fr034.htm.
8. Model I4G Interrogator. Info. available: www.faztechnology.com/products/interrogators/fazt-i4g/.
9. J. A. Sadler, "Fiber optic security system," U.S. Patent 4,292,628, Sep. 29, 1981, available: http://www.google.com/patents/US4292628.